BULLETIN OF THE POLISH ACADEMY OF SCIENCES
TECHNICAL SCIENCES, Vol. 74(3), 2026, Article number: e158298
DOI: 10.24425/bpasts.2026.158298

Instructional test bench for marine purpose diesel piston engines

Valentin PETRESCU[1], **Claudia SĂVESCU**[1,2], **Rareș CONȚIU**[1,2], **Sorin TOMESCU**[1], **Cristian NECHIFOR**[1]*, **Alexandru ȘERBAN**[1,2], and **Robert ISAC**[1,2]

[1] Romanian Research and Development Institute for Gas Turbines COMOTI, 061126 Bucharest, Romania
[2] National University of Science and Technology Politehnica Bucharest, Romania

Abstract. The paper presents the development of an instructional test bench designed to support the training of marine cadets in the operation and maintenance of tugboat propulsion systems powered by diesel engines. The test bench, developed by the authors and implemented at the Naval Academy "Mircea cel Bătrân" in Constanța, Romania, is intended to enhance practical understanding of propulsion system components and operating principles. The installation enables instruction on the construction and operation of four-stroke internal combustion engines, as well as on the correct monitoring of key parameters associated with a marine diesel engine, reversing gearbox, and hydraulic brake. Successive loading of the engine can be performed, allowing the analysis of engine behavior and power development under controlled operating conditions. The test bench comprises a diesel engine, reversing gearbox, axial shaft, and a downsized hydraulic brake coupled through a multiplier gearbox for emulating the propeller load. A custom-designed automation and control system is implemented, providing local and remote command consoles together with a replicating display for parameter monitoring. Auxiliary systems include compressed air supply, fuel storage and delivery, exhaust gas evacuation, cooling, and lubrication systems for both the engine and the brake.

Keywords: diesel piston engine; educational test bench; four-stroke combustion; marine propulsion; automation control.

1. INTRODUCTION

Test benches designed for simulating propeller loads in naval applications are essential for evaluating the performance of marine propulsion systems, particularly the diesel engines driving ship propellers and their couplings. By reproducing the resistive conditions encountered in real operating environments, such benches enable a controlled measurement of key parameters such as torque, speed, and efficiency.

Marine diesel engines [1–7] play a central role in maritime transportation, serving as main propulsion units as well as power sources for auxiliary systems [8]. Owing to their continuous operation under demanding mechanical and thermal conditions, these engines are subject to progressive wear and an increased likelihood of faults during service, underscoring the importance of reliable experimental and instructional test benches for performance evaluation, monitoring, and training.

Conventional diesel engine experimental setups frequently employ hydraulic (water-brake) dynamometers to absorb brake power and regulate load under steady-state conditions. Such configurations are widely adopted due to their robustness, ability to develop high torque, and suitability for continuous operation in marine environments. Research and laboratory facilities report marine diesel engines coupled to hydraulic dynamometers for performance characterization, fuel consumption analysis, and emission studies, both in instructional [9] and research oriented applications [1, 10, 11]. In these conventional setups, hydraulic brakes are chosen to manage the high torque at low rotational speeds downstream of marine reduction gearboxes, often resulting in large capacity dynamometers and auxiliary infrastructure requirements, including dedicated water handling systems and drainage solutions integrated into the laboratory layout.

Several studies address propulsion load simulation and experimental test benches for marine applications. Pan *et al.* [12] investigated propeller load simulation for marine electric propulsion systems, demonstrating generator load emulation for controlled torque application. Zhu *et al.* [13] discussed experimental testing approaches for marine diesel engines, emphasizing structured bench evaluation methods. Gabiña *et al.* [14] developed a full-scale marine diesel engine test bench where the engine was cooled with seawater and coupled to a hydraulic brake to simulate different propulsion loads and modes, including controllable and fixed pitch operation. Minchev *et al.* [10] reported a digital-twin of a marine diesel engine test bench, highlighting the potential of modern benches for advanced monitoring and model-based analysis. Vasile *et al.* [15] demonstrated propeller load simulation on a gas turbine test stand, confirming the relevance of controlled load reproduction in propulsion related experiments. Alternative load absorption solutions were also explored, such as the eddy current brake designed by Nunes and Brójo [16] for engine testing, which represents an electromagnetic approach suitable for specific operating regimes. From an educational perspective, Tărăbîc *et al.* [9] presented the modernization of a didactical piston engine test bench from analogue

*e-mail: cristian.nechifor@comoti.ro

Manuscript submitted 2025-11-28, revised 2026-02-03, initially accepted for publication 2026-02-22, published in May 2026.

to digital instrumentation, underlining the instructional value of enhanced measurement and control architectures. A related contribution by Săvescu *et al.* [17] detailed the automation and control architecture of an educational marine diesel engine test bench, including the PLC command logic, local and remote consoles, and parameter monitoring, highlighting the instructional instrumentation and supervisory control aspects.

In contrast to studies focusing primarily on load simulation principles or instrumentation upgrades, the present work addresses system-level instructional feasibility by introducing a multiplier gearbox within the hydraulic dynamometer architecture with a recirculated water management concept and a dual local/remote automation system, while experimentally validating that the bench preserves realistic diesel engine behavior under successive loading.

While instructional test benches are often described primarily from a technical implementation perspective, this paper formulates and verifies a design hypothesis relevant to marine propulsion training infrastructure.

The main contributions of this study are: (1) an integrated mechanical architecture for marine diesel instructional loading based on reduction + multiplier + hydraulic brake sizing; (2) a compact, recirculated water cooling system suitable for limited installation spaces; (3) an automation system and HMI solution with local and remote command consoles and replicated large display monitoring; and (4) quantitative validation using torque/speed power estimation and fuel consumption mapping under multiple load levels.

2. TEST BENCH DESIGN AND CONSTRUCTION

We propose an instructional bench integrating: (a) a compact load absorption architecture based on a speed multiplier gearbox enabling the selection of a smaller hydraulic dynamometer [9, 11, 15], (b) a closed-loop recirculated water reservoir eliminating civil works for an under-floor basin, and (c) a dual (local/remote) automation system mirroring real ship operation. The 3D CAD assembly is presented in Fig. 1.

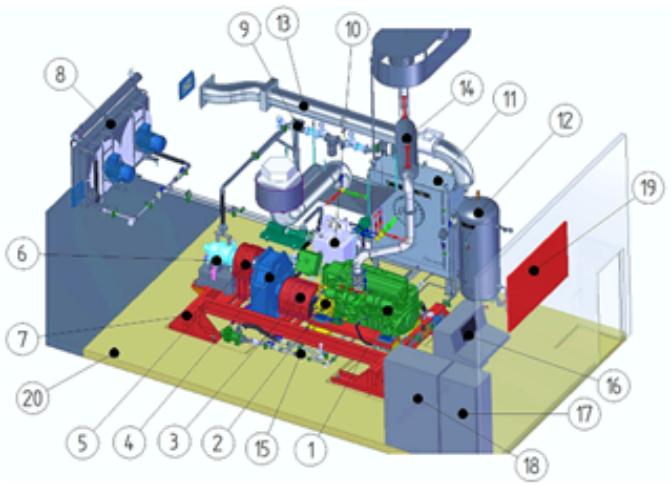

Fig. 1. 3D CAD model of the test bench

The main components integrated within the test bench, numbered in the figure above, are specified in Table 1.

Table 1
Main test bench components

No.	Test bench component
1.	Piston diesel engine, Volvo Penta D16
2.	Reverse reduction gearbox ($i = 2.06$), 2800GA-D-114CFR
3.	Cardan driveshaft
4.	Multiplier gearbox, $i = 3.06$
5.	Elastic coupling
6.	Hydraulic brake, Horiba DT900-2
7.	Frame assembly
8.	Heat exchanger, HPA 255
9.	Hydraulic brake circuit
10.	Multiplier gearbox oil lubrication circuit
11.	Fuel supply installation
12.	Compressed air installation
13.	Ventilation installation
14.	Discharge installation
15.	Engine cooling installation
16.	Command console (remote)
17.	Automation cabinet
18.	Drives cabinet
19.	Replicator display
20.	Room assembly

The selection of the engine and its reverse reduction gearbox resulted in challenges concerning the selection of an appropriate hydraulic brake. The reverse reduction gearbox imposes the use of a bidirectional hydraulic brake, capable of generating high torque at low rotational speeds. However, such a brake tends to be oversized, as it develops high torques at high speeds, and it also has an extremely inflated cost. To reduce the overall dimensions of the brake, a speed multiplier gearbox was introduced after the reverse reduction gearbox to increase the speed while simultaneously reducing the generated torque.

We hypothesize that our test bench for marine piston diesel engine [4, 18, 19] can provide functional and performance characteristics at least comparable to conventional instructional and experimental setups reported in the literature, while improving compactness, installation feasibility, and cost-efficiency. The hypothesis is supported by explicit identification of novelty elements versus state-of-the-art benches, as well as by experimental validation demonstrating stable operation and realistic engine behavior under successive loading, including power–speed consistency, partial-load power curves, and brake-specific fuel consumption trends consistent with expected diesel engine characteristics.

From an economic standpoint, hydraulic dynamometer sizing is primarily governed by the maximum torque to be absorbed, the costs increasing nonlinearly with torque capacity, particularly

for low-speed, high-torque operation. Because the multiplier gearbox increases the speed by ~ 3.1 times, the brake torque requirement drops by roughly the same factor. The hydraulic dynamometer cost tends to scale strongly with torque capacity and the heavy mechanical/thermal design that comes with it. In conventional direct-coupled configurations downstream of marine reduction gearboxes, the required dynamometer torque rating leads to significantly oversized braking units.

In our case, such a solution would have resulted in a braking system priced up to approximately four times higher than that of the smaller dynamometer chosen, operating at elevated rotational speed. By introducing a multiplier gearbox, the configuration shifts the operating point toward higher speed and lower torque, enabling substantial reductions in equipment size and overall system costs, while maintaining the same functional performance.

The kinematic chain introduces additional design constraints related to the operating range of the selected hydraulic dynamometer. The reduction gearbox transmission ratio ($i = 2.06$) is imposed by the propulsion configuration that the test bench emulates. The multiplier gearbox ratio ($i = 3.06$) was selected to shift the operating point of the hydraulic dynamometer towards its optimal rotational speed range, where stable torque and measurement accuracy are ensured. This configuration allows reliable load control while avoiding oversizing of the braking unit required to directly absorb high torque at low rotational speeds.

In Fig. 2, the specified torque generated by the engine (M_{motor}) is represented in blue, the torque after the reverse reduction gearbox (M_{red}) is shown in red, the torque after the speed multiplier (M_{dyno}) is represented in green, and the maximum torque that can be generated by the brake ($M_{\text{max\_dyno}}$) is illustrated in yellow. The torque output after the reverse reduction gearbox is high at low rotational speeds. Consequently, a hydraulic brake capable of covering this range would be oversized for this application.

Generally, hydraulic brakes operate more efficiently at higher rotational speeds, around 1500–2000 rpm. The multiplier gearbox shifts the operating point toward higher speeds and lower torque, thus avoiding oversizing of the hydraulic brake required to directly absorb high torque at low speeds.

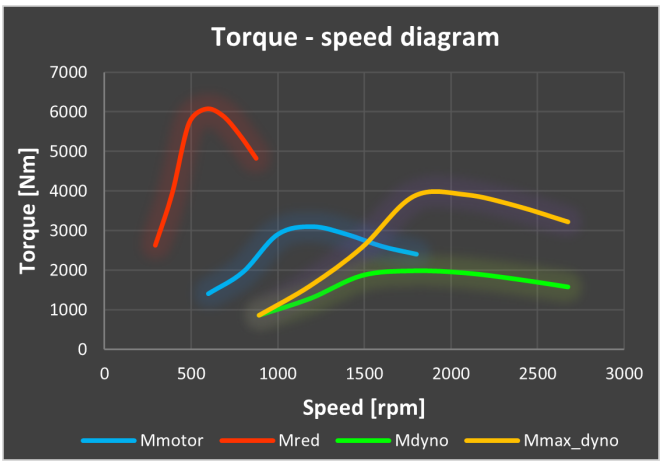

Fig. 2. Torque variation along the kinematic chain as a function of rotational speed

The physical test bench is presented in Fig. 3. The main elements of the kinematic chain are as follows: the diesel engine Penta D16, the reverse reduction gearbox DMT280H with the reduction ratio $i = 2.06$, the multiplier gearbox CHP220 with the multiplication ratio $i = 3.06$, and the hydraulic brake.

Fig. 3. The diesel engines test bench

Figure 4 shows a 3D CAD isometric view of the entire naval engines test bench, integrating all the components and subsystems.

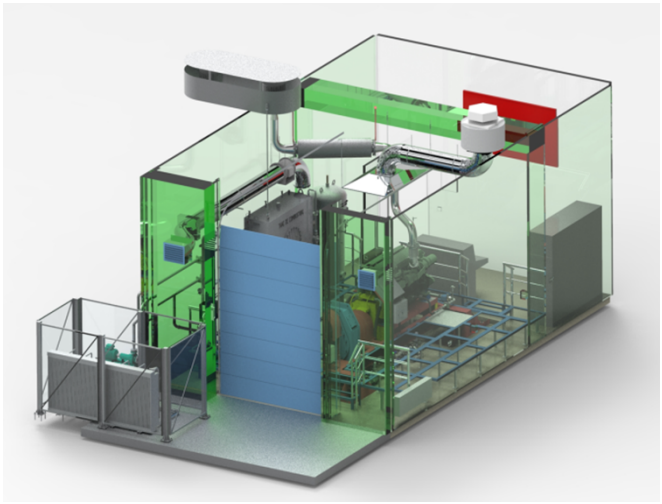

Fig. 4. Isometric view of the diesel engine test bench

The Horiba DT type hydraulic dynamometer converts the mechanical energy of the engine, derived from torque and rotational speed, into heat, which is subsequently dissipated into water. During this process, the water serves both as a working medium for generating braking torque and as a cooling agent for dissipating the kinetic energy transformed into heat. The supplied cooling water is introduced into the hydraulic dynamometer, where it is accelerated by the dynamometer rotor.

One of the challenges in developing the test bench was the limited amount of water available for the brake. For this application, a 5 m^3 reservoir (Fig. 5) had to be used, from which the water had to be recirculated. Additionally, when installing a hydraulic brake, a separate water reservoir was positioned underneath the brake to allow the water to freely drain from the brake into the reservoir (the brake operates on the pressure rupture bar). Given the narrow space for installing the reservoir, a system with two water pumps [20] was chosen. The first pump draws water from the 5 m^3 reservoir and supplies it to the hydraulic brake; the second pump intakes the water directly from the hydraulic brake reservoir and returns it to the main reservoir.

Fig. 5. The water reservoir

3. AUTOMATION CONTROL SYSTEM

The automation system comprises a drives cabinet, an automation cabinet, two control consoles for local and remote commands, as well as a large display replicating the screen displayed on the Panel PC of the remote console. A 98" diagonal display is mounted on the wall behind the remote console, so that the parameters can be followed easily by the staff, trainees, and/or students.

The drives and automation cabinets are presented in Fig. 6. The drives cabinet, which has two doors, comprises three frequency inverters: one for the air fan that cools the engine, one for the pump for water recirculation that also cools the engine, and one for the water retour pump of the brake. The motor speed control of the pump depends on the water level in the tank placed under the brake, where the water from the brake drains and is stored.

Fig. 6. Control cabinets – drives and automation sections

The automation cabinet is equipped with a VersaMax PLC (programmable logic controller), which includes the following CPU (central processing unit) and I/O (input/output) modules: three 15-channel analogue input modules, one 8-channel analogue output module, one 32-channel digital input module, one 32-channel digital output module, and six module carriers for the I/O modules. The custom software is designed in the Proficy Machine Edition ladder diagram.

The remote command and control console (Fig. 7) simulates the command console located on the deck of ships. It is provided with a touchscreen operator panel for controlling the entire test bench, including a lever and control screen for the engine, also embedding computers for hydraulic brake.

The local command and control console (Fig. 8) simulates the command console located in the engine room, on board naval ships. It includes a lever for engine speed control, the engine start-up screen and buttons, as well as an emergency shutdown button. From the local console, only the engine can be controlled. It is equipped with a covered screen, on which the essential parameters are displayed as clocks, replicating the way information is presented on board of ships.

Fig. 7. Control cabinets – drives and automation sections

Fig. 8. Local command console

4. RESULTS AND DISCUSSION

The test bench operates in good conditions, as demonstrated by the parameters displayed on the screen in Fig. 9 falling within the normal operating ranges. The parameters with their legend are listed in Table 2.

Table 2
Parameters abbreviations legend

No.	Parameter [Unit]	Legend
Engine start-up installation		
1.	Paer_R [bar]	Air pressure in the reservoir
2.	Paer_M [bar]	Start-up air pressure
Engine related installations		
3.	Ncb [mm]	Fuel level
4.	Tcb [°C]	Fuel temperature
5.	Qcb_t [L/h]	Fuel flow in
6.	Qcb_r [L/h]	Fuel flow out
7.	Qcb [L/h]	Fuel flow engine consumption
8.	Egt1 [°C]	Exhaust gas temperature
9.	Par_M [bar]	Cooling water pressure
10.	fTar_M [°C]	Cooling water temperature
11.	Pu_M [bar]	Engine oil pressure
12.	NVSD1 [rpm]	Antifreeze pump speed
13.	NVSD3 [rpm]	Cooling fan speed
Enclosure ventilation installation		
14.	Taer_B [°C]	Ambient air temperature
15.	Vap_B [%LEL]	Fuel vapors detector
16.	CO2_B [ppm]	Carbon dioxide detector
17.	CO_B [ppm]	Carbon monoxide detector
Brake cooling installation		
18.	Par_iF [bar]	Brake water pressure, before regulator
19.	Par_F [bar]	Brake water pressure, after regulator
20.	Tar_iF [°C]	Brake inlet water temperature
21.	Tar_dF [°C]	Brake outlet water temperature
22.	%d_F [%]	Brake positioning valve
23.	Nm_F [Nm]	Brake resistive torque
24.	n_F [rpm]	Brake speed
25.	Nar_F [mm]	Brake water level
26.	W_F [kW]	Brake power
27.	Wh_F [hP]	Brake power (horsepower)
28.	NVSD2 [rpm]	Water flow-off pump speed
Multiplier gearbox lubrication installation		
29.	Pu_Mt [bar]	Multiplier gearbox oil pressure
30.	Tu_Mt [°C]	Multiplier gearbox oil temperature

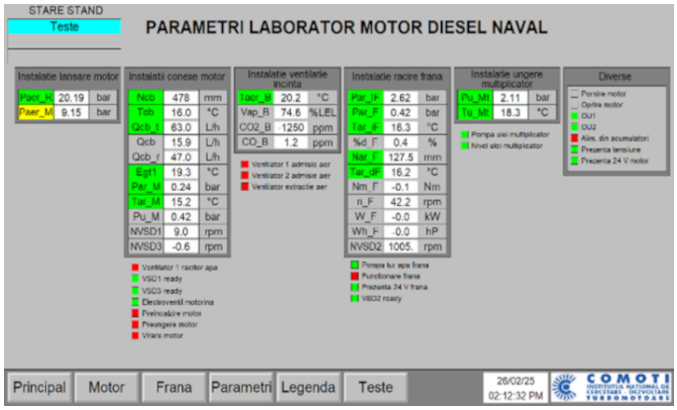

Fig. 9. Engine parameters displayed on screen

Considering that we cannot measure the engine power directly, we calculated it using equation (1), and relying on the measured torque and rotational speed, while accounting for gearbox efficiencies. The measured and theoretical powers at 100% load follow a similar trend, with remarkably close values (Fig. 10). The close agreement between the calculated and measured values (maximum relative error ≈ 6%) validates the torque–speed-based power estimation approach.

$$P_{\text{engine}} = \frac{M_{\text{dyno}} \cdot \omega}{\eta_{\text{red}} \cdot \eta_{\text{multi}}}, \tag{1}$$

where P_{engine} [kW] – engine power; M_{dyno} [Nm] – brake torque; ω [rad/s] – angular velocity; $\eta_{\text{red}} = 0.98$ [ND] – reduction gearbox efficiency; $\eta_{\text{multi}} = 0.98$ [ND] – multiplier gearbox efficiency.

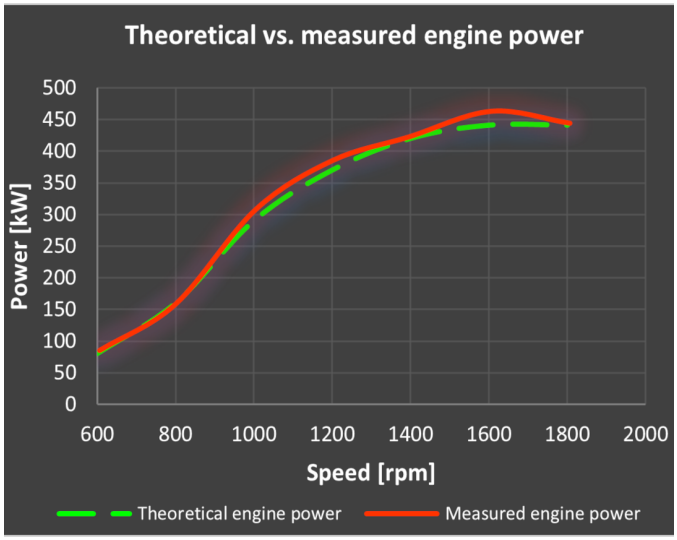

Fig. 10. Comparison between calculated engine power and measured resistive power at 100% load, being in close agreement

The same speed values were used to calculate the engine power at various partial loads (50%, 60%, 70%, 80%, 90%, 100%). Given the acceptable computation error from measured values, the computation formulae were deemed reliable to use for further determining the engine power at partial loads (Fig. 11).

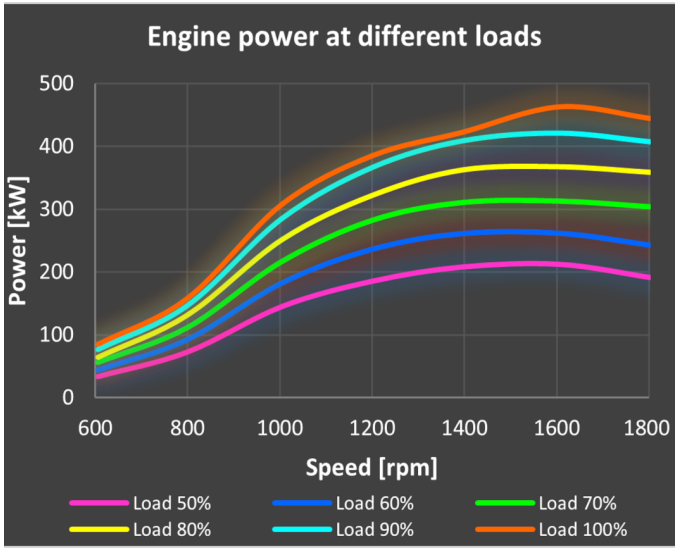

Fig. 11. Calculated engine power at different simulated load levels (50–100%), demonstrating consistent power–speed behavior

The fuel consumption was calculated with equation (2):

$$c_e = \frac{c_{cb}}{P_{\text{engine}}} \cdot 1000, \tag{2}$$

where c_e [g/kWh] – brake-specific fuel consumption; c_{cb} [kg/h] – fuel mass flow rate (measured); P_{engine} [kW] – engine power at each speed level.

Considering that the fuel flow is measured using a volumetric flowmeter, and not a mass flowmeter, the mass flow rate was calculated with relation (3), using the diesel density of $\rho_{\text{diesel}} = 876$ kg/m^3. The volumetric flows $c_{cb_{\text{in}}}$ and $c_{cb_{\text{out}}}$ are acquired by PLC as Qcb_t and Qcb_r parameters, respectively.

$$c_{cb} = \left(c_{cb_{\text{in}}} - c_{cb_{\text{out}}}\right) \cdot \rho_{\text{diesel}}, \tag{3}$$

where c_{cb} [kg/h] – fuel mass flow rate; $c_{cb_{\text{in}}}$ [L/h] – fuel flow in (Qcb_t); $c_{cb_{\text{out}}}$ [L/h] – fuel flow out (Qcb_r); ρ_{diesel} [kg/m^3] – diesel fuel density.

The graph in Fig. 12 plots the fuel consumption at various partial loads of the engine, known as the brake-specific fuel consumption (BSFC). The peak engine efficiencies for all partial loads were recorded at around 1200 rpm, which corresponds to the maximum torque produced by the engine. This is a consequence of the usual behavior of all internal combustion engines, where it is normal that the highest torque results in the highest engine efficiency. Minimum BSFC values are observed around 1200 rpm, corresponding to the maximum torque region of the engine, which is consistent with typical diesel engine behavior.

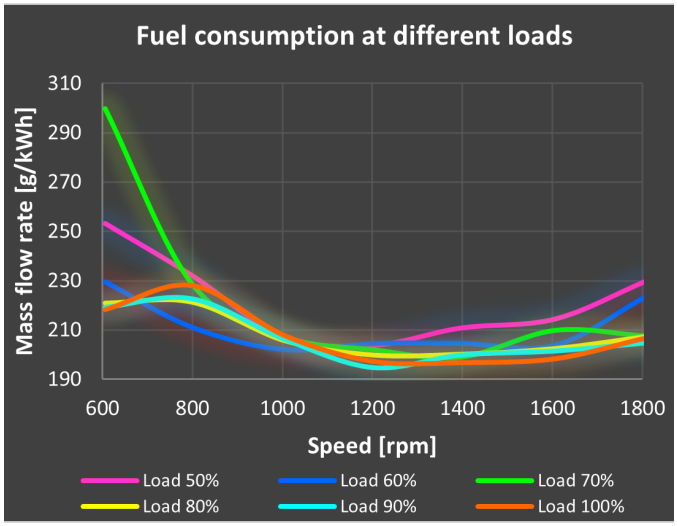

Fig. 12. Brake-specific fuel consumption (BSFC) as a function of rotational speed for different load levels

5. CONCLUSIONS

The test bench designed and developed for naval diesel engines showed good and reliable operation and proved its usefulness for the practical marine laboratory work. The solution brings some original elements, such as the water reservoir, which eliminates the need for digging a basin under the brake, as is customarily practiced.

The test bench presented herein was developed by our team within a contract with the Naval Academy "Mircea cel Bătrân", Constanța (beneficiary). This one will be able to demonstrate to both the institutional monitoring and evaluation committees of Romanian Navy authorities that its resources meet the quality standards imposed, ensuring that training meets the high-level requirements. The test bench is a useful educational tool for the defense industry.

The present work follows the hydraulic brake testing paradigm while proposing a modified transmission and water management architecture aimed at reducing brake oversizing and installation constraints in instructional laboratories.

From an economic perspective, the proposed solution addresses two dominant cost drivers of instructional hydraulic-brake test benches: the capacity of the braking unit and the associated installation infrastructure. The introduction of the multiplier gearbox enabled the selection of a smaller capacity hydraulic dynamometer compared to conventional direct-coupled solutions, while the recirculated water reservoir eliminated the need for civil works related to under-floor drainage basins. These measures reduce both initial investment and installation costs. In a small-series production scenario, additional – though comparatively less significant – cost reductions are expected through the standardization of the automation cabinet, control interfaces, and instrumentation. Further savings may arise from reduced engineering and integration effort, as preliminary design activities and extensive market analysis for equipment selection would no longer be required.

The multiplier gearbox we introduced in the kinematic chain elevates the speed to match the required value in the scope of work, which allowed us to choose a smaller brake. This came with benefits regarding the compactness of the solution, as well as reducing the costs for an oversized brake. The results demonstrate a stable successive loading and consistent power–speed behavior, confirming the suitability of the test bench for instructional analysis of partial-load operation.

Future work will include fault simulation and troubleshooting scenarios, as well as determining the characteristics of the diesel engine for various kinds of propeller loads. The integration of a communication module for acquiring engine parameters is also envisaged, ensuring that the system replicates the configuration used on real diesel-powered tugboats.

ACKNOWLEDGEMENTS

The research reported in this paper was conducted within the Romanian Research and Development Institute for Gas Turbines COMOTI, as part of contract AP16115/06.12.2023 "Naval Diesel Engines Laboratory", for the Naval Academy "Mircea cel Bătrân" in Constanța, as beneficiary.

We would like to thank our colleague, Adrian Săvescu, who provided important insights regarding the automation system and test bench operation.

REFERENCES

[1] M. Palocz-Andresen, "Marine Diesel Engines," in *Decreasing Fuel Consumption and Exhaust Gas Emissions in Transportation: Sensing, Control and Reduction of Emissions*, M. Palocz-Andresen, Ed., Berlin, Heidelberg: Springer, 2013, pp. 159–172, doi: 10.1007/978-3-642-11976-7_11.

[2] J.B. Woodward and T.E. Andersen, "Marine Engines," in *Encyclopedia of Physical Science and Technology (Third Edition)*, R.A. Meyers, Ed., New York: Academic Press, 2003, pp. 121–132, doi: 10.1016/B0-12-227410-5/00404-X.

[3] J. Castresana, G. Gabiña, L. Martin, A. Basterretxea, and Z. Uriondo, "Marine diesel engine ANN modelling with multiple output for complete engine performance map," *Fuel*, vol. 319, p. 123873, Jul. 2022, doi: 10.1016/j.fuel.2022.123873.

[4] J.P. Gregório and F.M. Brójo, "Development of a 4 stroke spark ignition opposed piston engine," *Open Engineering*, vol. 8, no. 1, pp. 337–343, Jan. 2018, doi: 10.1515/eng-2018-0039.

[5] M. Okubo and T. Kuwahara, "Chapter 5 – Prospects for marine diesel engine emission control," in *New Technologies for Emission Control in Marine Diesel Engines*, M. Okubo and T. Kuwahara, Eds., Butterworth-Heinemann, 2020, pp. 211–266. doi: 10.1016/B978-0-12-812307-2.00005-5.

[6] A. Chakraborty, S. Roy, and R. Banerjee, "An experimental based ANN approach in mapping performance-emission characteristics of a diesel engine operating in dual-fuel mode with LPG," *J. Nat. Gas Sci. Eng.*, vol. 28, pp. 15–30, Jan. 2016, doi: 10.1016/j.jngse.2015.11.024.

[7] M. Noga and S. Bronislaw, "Increase of efficiency of SI engine through the implementation of thermodynamic cycle with additional expansion," *Bull. Pol. Acad. Sci. Tech. Sci.*, vol. 62, no. 2, pp. 349–355, 2014, doi: 10.2478/bpasts-2014-0034.

[8] M. Borzea, G. Fetea, and R. Codoban, "Implementation and Operation of a Cogeneration Plant for Steam Injection in Oil Field," in *ASME Turbo Expo 2008: Power for Land, Sea, and Air*, American Society of Mechanical Engineers Digital Collection, Aug. 2009, pp. 137–146, doi: 10.1115/GT2008-50518.

[9] C.M. Tărăbîc, G. Cican, G. Dediu, and R.M. Catană, "Updating a Didactical Piston Engine Test Bench, from Analogue Instrumentation to Digital," *Tehnički vjesnik*, vol. 31, no. 4, pp. 1087–1094, Jun. 2024, doi: 10.17559/TV-20230315000440.

[10] D. Minchev *et al.*, "Digital twin test-bench performance for marine diesel engine applications," *Pol. Marit. Res.*, vol. 30, no. 4, pp. 81–91, Dec. 2023, doi: 10.2478/pomr-2023-0061.

[11] N.A. Visan, D.C. Niculescu, R. Ionescu, E. Dahlin, M. Eriksson, and R. Chiriac, "Study of Effects on Performances and Emissions of a Large Marine Diesel Engine Partially Fuelled with Biodiesel B20 and Methanol," *J. Mar. Sci. Eng.*, vol. 12, no. 6, p. 6, Jun. 2024, doi: 10.3390/jmse12060952.

[12] J. Pan, Y. Yunan, and F. Shidong, "Simulation for the propeller loading of marine electrical propulsion based on matlab," in *2011 International Conference on Electric Information and Control Engineering*, Apr. 2011, pp. 2587–2591, doi: 10.1109/ICEICE.2011.5777018.

[13] M. Zhu, G. Chen, Z. Liu, T. Liu, S. Su, and Y. Cao, "Study on the Testing Method for Marine Diesel Engine," *Indones. J. Electr. Eng. Comput. Sci.*, vol. 12, no. 2, p. 2, Feb. 2014, [Online]. Available: https://ijeecs.iaescore.com/index.php/IJEECS/article/view/3092 (Accessed: Mar. 11, 2025).

[14] G. Gabiña, L. Martin, O.C. Basurko, M. Clemente, S. Aldekoa, and Z. Uriondo, "Performance of marine diesel engine in propulsion mode with a waste oil-based alternative fuel," *Fuel*, vol. 235, pp. 259–268, Jan. 2019, doi: 10.1016/j.fuel.2018.07.113.

[15] M.L. Vasile, G. Dediu, F. Niculescu, C.I. Borzea, and G. Balan, "Propeller load simulation on gas turbine test stand," in *2022 International Conference on Electrical, Computer and Energy Technologies (ICECET)*, Jul. 2022, pp. 1–5, doi: 10.1109/ICECET55527.2022.9872833.

[16] A.J.R. Nunes and F.M.R.P. Brojo, "Designing an Eddy Current Brake for Engine Testing," *KEG*, vol. 5, no. 6, pp. 743–756, Jun. 2020, doi: 10.18502/keg.v5i6.7094.

[17] C. Săvescu *et al.*, "Automation System of an Educational Test Bench for Naval Piston Diesel Engines," *Rev. Roum. Sci. Techn. – Électrotechn. et Énerg.*, vol. 70, no. 4, pp. 597–602, Nov. 2025, doi: 10.59277/RRST-EE.2025.4.29.

[18] A. Bąkowski and L. Radziszewski, "Determining selected diesel engine combustion descriptors based on the analysis of the coefficient of variation of in-chamber pressure," *Bull. Pol. Acad. Sci. Tech. Sci.*, vol. 63, no. 2, pp. 457–464, 2015, doi: 10.2478/bpasts-2014-0034.

[19] M. Bednarski, P. Orlinski, M. Wojs, and M. Gis, "Evaluation of the heat release rate during the combustion process in the diesel engine chamber powered with fuel from renewable energy sources," *Bull. Pol. Acad. Sci. tech. Sci.*, vol. 68, no. 6, pp. 1333–1339, 2020, doi: 10.24425/bpasts.2020.135394.

[20] D. Dima, A. Dobrovicescu, C. Ioniţă, and C. Dobre, "Exergy analysis of the coupling of two CO2 heat pump cycles," *Rev. Roum. Sci. Techn. – Électrotechn. et Énerg.*, vol. 68, no. 2, pp. 236–240, Jul. 2023, doi: 10.59277/RRST-EE.2023.68.2.20.